

Liquid circulation rates in two- and three-phase external airlift reactors

Renzo Di Felice*

Dipartimento di Ingegneria Chimica e di Processo G.B. Bonino, Università degli Studi di Genova, Via Opera Pia 15, 16145 Genova, Italy

Received 4 January 2005; received in revised form 2 March 2005; accepted 8 March 2005

Abstract

The dependency of the main parameters of an airlift reactor on the only externally adjustable factor, the gas flow rate, has been investigated both experimentally and theoretically for two-phase (gas–liquid) and three-phase (gas–liquid–solid) systems. Experiments were performed on external airlift arrangements employing ambient air, tap water and, for the three-phase case, glass spheres. The pressure drop balance has been the basis for the theoretical predictions. The simple rig and the low gas hold-ups utilised in this work have permitted an accurate prediction of friction losses (both concentrated and distributed) based exclusively on well established relationships published in the literature, without resort to any fitting parameters; this has resulted in estimates in very good agreement with measured values.

© 2005 Elsevier B.V. All rights reserved.

Keywords: Airlift systems; Liquid circulation rate; Fluid dynamics; Pressure drop

1. Introduction

Airlift systems represent a very convenient technical solution for cases where liquid circulation needs to be achieved, like in biotechnological applications, with a limited or no use at all of any mechanical device. The system is made up of two separate sections, a riser and a downcomer. In the riser, gas is blown in at the bottom, resulting in a difference in static pressure in the two sections brought about by the different concentrations of the gas phase; this results in an overall circulation of the liquid and, depending on the operating parameters, also of part of the gas. Specific applications may require the presence of a solid phase also, which is charged in the riser column and again, depending on the operating parameters, could form a packed bed at the base of the column, be fluidised in the riser or, for the extreme case, circulate in the system. These various modes of operation have already been classified [1] for a draft tube system but that classification can be equally applied to external airlift reactors and will not be repeated here.

The fluid dynamic compartment of these systems has been studied for many years now, starting with the work of Hsu

and Dudukovic [2], Bello et al. [3] and Chisti et al. [4] for the two-phase gas–liquid systems, and with the work of Livingston and Zhang [5] and Freitas et al. [6] for the three-phase, gas–liquid–solid systems, all based on overall momentum balance. On the other hand the approaches suggested by Garcia Calvo [7] for the two-phase and Garcia Calvo et al. [8] for the three-phase are based on an energy balance of the airlift system, although its final results are not very dissimilar from other studies. In recent years computational fluid dynamic (CFD) codes have also come to be increasingly applied to the detailed description of the airlift system behaviour [9]. In spite of the clear *qualitative* correspondence of these simulations with observed behaviour, confidence in their *quantitative* predictions is somewhat limited by the absence of a complete description of the basic fluid dynamic phenomena governing the whole system. A full numerical simulation becomes a necessity for an insight of the local behaviour of a multiphase system, but when we are interested primarily in some overall characteristics then perhaps a more basic approach is to be preferred. In this work a basic study has been carried out with a simple objective in mind: to characterise the overall behaviour of an airlift reactor system, with particular reference to the liquid circulation rate, operating with or without the presence of a solid phase, on the basis of well estab-

* Tel.: +39 010 3532924; fax: +39 010 3532586.

E-mail address: difelice@dichep.unige.it.

Nomenclature

A	area, m ²
d	particle diameter, m
D	column diameter, m
g	acceleration of gravity, m/s ²
f	friction factor, –
H	column height, m
K	concentrated friction factor
L	distance, m
n	numerical parameter in the Richardson–Zaki equation
P	pressure, Pa
Q	circulation rate, m ³ /s
W	solid charged in the riser, kg

Greek letters

ε	phase volume fraction, –
ρ	density, kg/m ³
μ	viscosity, kg/m/s

Subscripts

C	concentrated
D	distributed
dc	downcomer
G	gas
L	liquid
mf	minimum fluidisation
r	riser
S	solid

lished, general relationships containing no ad hoc adjustable parameters.

2. Pressure balance of an airlift reactor

The difference in weight in the two vertical columns of the airlift reactor provides the driving force for the liquid circulation; under steady state this driving force has to be balanced by losses due to the flow itself. The basis of the approach as stated here is certainly not new, having been that of many previous workers, including [4,5,10–12].

We start by considering a well-defined situation typical of relatively low gas flow rates: gas and solid phases are present only in the riser column with the solid in a fluidised state occupying a height H_S of the total airlift height H . The driving force, i.e. the difference in weight in the two vertical columns expressed in term of pressure difference, is given then by

$$\Delta P = H\rho_L g - H_S[\varepsilon_S \rho_S + (\varepsilon_G \rho_G + \varepsilon_L \rho_L)(1 - \varepsilon_S)]g - (H - H_S)(\varepsilon_L \rho_L + \varepsilon_G \rho_G)g \quad (1)$$

In Eq. (1) P is the piezometric pressure, and this pressure will be utilised for simplicity in the rest of the paper. Eq. (1) has been written with the simplifying assumption that the relative volume fraction between the gas and liquid in the riser is constant regardless of the presence of the solid phase. By introducing in Eq. (1) the solid loading W , i.e. the mass of solid charged in the column

$$W = H_S A_R \rho_S \varepsilon_S \quad (2)$$

and neglecting gas density relative to liquid and solid density we obtain

$$\Delta P = H\rho_L \varepsilon_G g - \frac{W}{A_R} \left(1 - \varepsilon_L \frac{\rho_L}{\rho_S}\right) g \quad (3)$$

The driving force is therefore made up of two contribution, of different sign. The first, ΔP_G , brought about by the presence of the bubbles in the fluid phase

$$\Delta P_G = H\rho_L \varepsilon_G g \quad (4)$$

and the second, ΔP_S , brought about by the presence of the solid phase

$$\Delta P_S = -\frac{W}{A_R} \left(1 - \varepsilon_L \frac{\rho_L}{\rho_S}\right) g \quad (5)$$

The above relationships apply, as already said, when no circulation exist for the dispersed phases and when the solid is fluidised. Their extension to the case where gas and solid are circulating in the system is quite straightforward in principle. If gas is circulating then Eq. (4) should be written with the difference of gas volume fraction between riser and downcomer instead of ε_G simply, and analogously if solid is present in both sections then Eq. (5) should consider the difference of solid weight in the two halves of the system rather than simply W . How to estimate gas and solid volume fraction in the downcomer is beyond the scope of the present work (a possible approach allowing the determination of the fraction of circulating gas has been suggested in [13]) and will be dealt with in a future paper. For the time being we limited ourselves here to cases where only liquid is present in the return column.

For the solid in the fixed rather than in fluidised state, at a volume concentration of 0.6, the Ergun equation suffices instead of Eq. (5):

$$\Delta P_S = \frac{W}{\rho_S A_r} \left[\frac{1406\mu_L}{d^2} \left(\frac{Q_L}{A_r}\right) + \frac{27.3\rho_L}{d} \left(\frac{Q_L}{A_r}\right)^2 \right] \quad (6)$$

(the numerical routine adopted in this work utilises either Eqs. (5) or (6) depending on which one yields a lower value of pressure drop for the given operating condition).

Liquid circulation is resisted by friction losses, made up of distributed ΔP_D (due to wall effects), and concentrated ΔP_C (acceleration of the liquid phase).

Distributed pressure losses, ΔP_D , originate from the friction between the fluid phase and column wall, both in the riser and in the downcomer. The fluid phase is a gas–liquid

mixture but, given that the gas fraction is always rather small, single-phase equations can be used to good approximation:

$$\Delta P_D = \frac{1}{2} H \rho_L \left[\frac{f_r}{D_r} \left(\frac{Q_L}{A_r} \right)^2 + \frac{f_{dc}}{D_{dc}} \left(\frac{Q_L}{A_{dc}} \right)^2 \right] \quad (7)$$

For the friction factor f the well-known correlation for flow in pipes has been used [14]:

$$f = \frac{0.316}{Re^{0.25}} = \frac{0.316}{(Q_L \rho_L / D \mu_L)^{0.25}} \quad (8)$$

Concentrated pressure losses, ΔP_C , are, in this case, due exclusively to liquid acceleration and deceleration at the entrance and the exit of both the riser and downcomer columns:

$$\Delta P_C = \frac{1}{2} K_r \rho_L \left(\frac{Q_L}{A_r} \right)^2 + \frac{1}{2} K_{dc} \rho_L \left(\frac{Q_L}{A_{dc}} \right)^2 \quad (9)$$

where K_r and K_{dc} may be estimated from Fig. 8.15 of [14], taking the values 1.2 and 0.4, respectively, for the specific experimental apparatus utilised in this work.

In order to numerically determine the dependency of the liquid circulation rate on the gas flow rate from the above equations, a relationship is needed linking liquid and gas velocity and gas volume fraction in the riser. This is given by the equation suggested in [5], with the original constant of 0.45 replaced here by 0.25 to take into account that we are in bubbly rather than in heterogeneous flow regime:

$$\varepsilon_G = \frac{Q_G / A_r}{0.25 + 1.1(Q_G / A_r + Q_L / A_r)} \quad (10)$$

In summary, we are able to predict by using the above reported relationships the value of liquid circulation rate as a function of the gas flow rate once all the characteristics of the airlift system have been defined.

In order to completely define the compartment of the airlift system we need to estimate how much of the riser is occupied by the fluidised solid. The solid is suspended by a gas–liquid mixture and its expansion can be calculated by using the pseudo-fluid simplification which has proved successful when applied to three-phase fluidisation [15]. Again considering the gas hold-up would make little impact so that a single-phase approach as the Richardson and Zaki [16] equation

$$\varepsilon_S = 1 - \left(\frac{u}{u_t} \right)^{1/n} = 1 - \left(\frac{Q_L}{A_r u_t} \right)^{1/n} \quad (11)$$

can then simply be applied allowing the determination on ε_S and, consequently, H_S .

Needless to say, a calculated value of H_S greater than the column height H would indicate that the solid is circulating in the system.

3. Experimental

Experiments were carried out using the following experimental setup shown in Fig. 1. It consists of two transparent square section vertical columns whose sides measured 50 and 100 mm; the particular modular design allowed for the height to be easily changed, and here two working heights, of 1 and 2 m, respectively, were utilised. The columns are connected at the base by a large chamber, and at the top by an open wide channel, which provides for complete gas disengagement (so that no gas bubbles can enter the downcomer leg) and liquid circulation. The system was filled up to half the height the connection channel with tap water. Ambient air, from the laboratory line, was fed to the bottom of the smaller, riser column via a small tube fitted with a porous distributor at its centre. Airflow rates were regulated with a precision needle valve and measured with a ball rotameter. Water velocity in the downcomer, and consequently the liquid circulation rate, was measured by means of an electromagnetic sensor (ACM250-D, Alec Electronics, Japan) placed in the core of the flux, in the bottom half of larger column. The sensor is set to obtain data at 2 s intervals for a period of 5 min, so that the water velocity in the downcomer is obtained as the average of 151 measurements. Pressure taps were placed along the walls of the smaller diameter column, and connected via

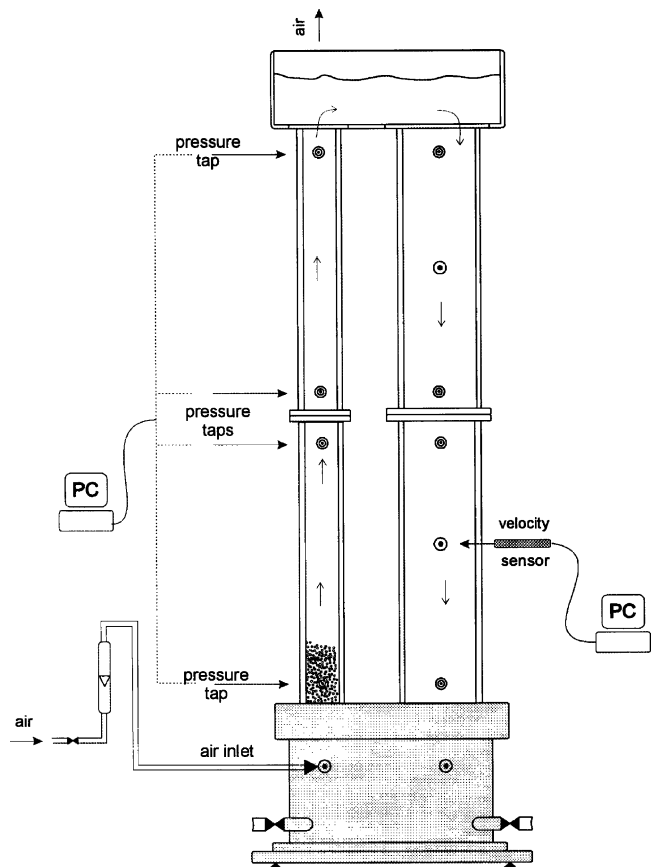


Fig. 1. Schematic representation of the experimental airlift reactor used.

a piezometric differential pressure transducer to a data acquisition system. Pressure sampling was carried out for 20 s periods at a rate of 20 Hz. Differential pressure measurements were used to infer the gas volume concentration through the following relationship:

$$\varepsilon_G = \frac{(\Delta P/L)_{\text{exp}}}{(\rho_L - \rho_G)g} \quad (12)$$

The use of Eq. (12) implies that the piezometric pressure gradient is due exclusively to the presence of the gas phase in the column. This is obviously not completely correct as the friction at the wall column between the fluid and the solid boundary also contribute to some extent to this loss in the riser, in a way that Eq. (12) underestimates the gas volume fraction. However, we verified that the contribution of the friction on the wall was always small compared to the overall measured pressure drop.

The behaviour of the airlift system was investigated, first by considering only the two-phase gas–liquid system, then with the addition of different amounts of 5 mm soda glass particles to the riser. During the runs, the conditions were such that the solid always remained in the riser column: it was either in the fixed or the suspended, fluidised state, the transition from one regime to the other being clearly visible. When fluidised, solid bed expansion was also very easily estimated visually.

4. Results and discussion

The first set of experiments involved simply the investigation of a two-phase, air–water, system. Air was bubbled in at the bottom of the riser and the liquid circulation rate, together with the average gas-hold up, was measured. It was first of all verified that the measured pressure drop would indicate, with very good approximation, gas phase volume fraction in the riser column. Fig. 2 reports, for any gas flow rate investigated, the ratio between the calculated pressure due to fluid-wall friction (ΔP_D) to the measured value. It is evident that for all the cases investigated friction losses never contribute more than 10% to the overall pressure drop; therefore the error in estimating ε_G was never larger than that percentage.

The results for the liquid circulation rates are summarised in Fig. 3 for the two column heights used. They confirm that as the gas flow rate increases so does the liquid circulation rate, roughly in an exponential manner. Also that the liquid circulation rate increases for a fixed gas flow rate when column heights are increased, as is to be expected – although the relation is not a directly proportional one. The same figure reports predictions for Q_L , obtained using the relationships given in the previous section. The agreement between experimental and calculated values appears excellent, in particular when it is considered that no adjustable factors have been employed. One of the important assumptions at the basis of the predictive model is the validity of the Hills equation for

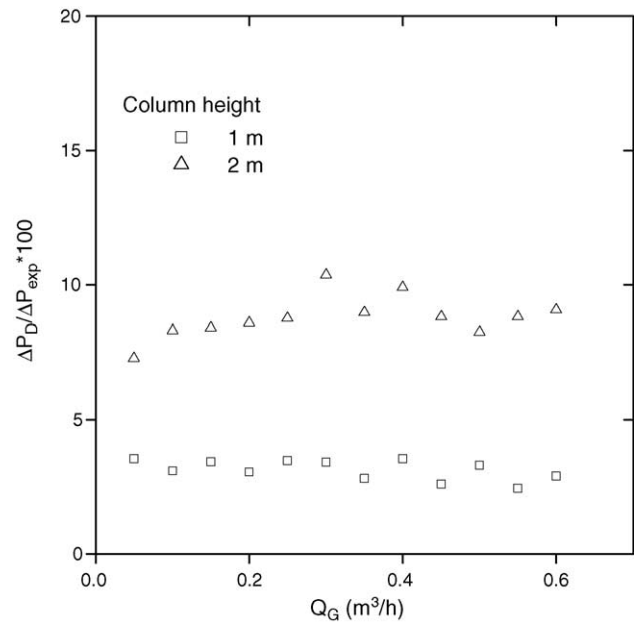


Fig. 2. Ratio of calculated pressure drop due to wall friction to overall measured value.

gas–liquid flow in the riser. This was confirmed by comparing measured and calculated gas volume fractions for each operating condition, as shown in Fig. 4.

The relative magnitude of the resistances to fluid flow for the present airlift arrangement has also been investigated. The ratio of distributed pressure losses to overall pressure losses is reported in Fig. 5 for the two column heights used. It is evident that both distributed and concentrated pressure losses are important, the two contributions being approximately equal for the 2 m columns. As, by changing column

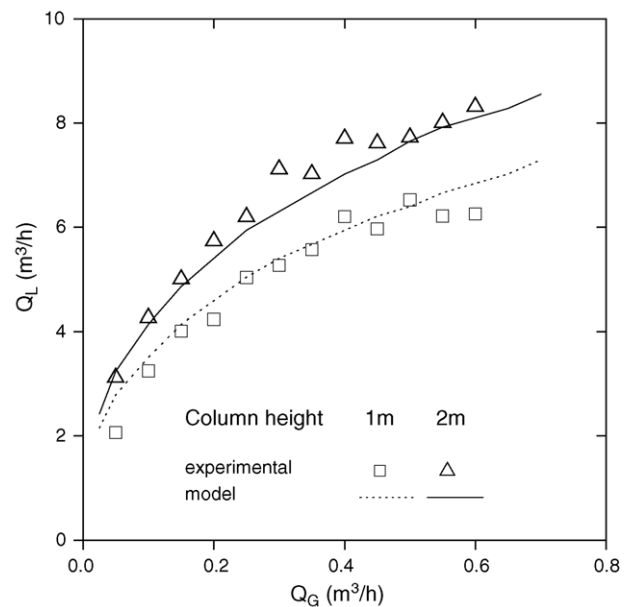


Fig. 3. Experimental and calculated liquid circulation rate function of gas flow rate. Two-phase gas–liquid system.

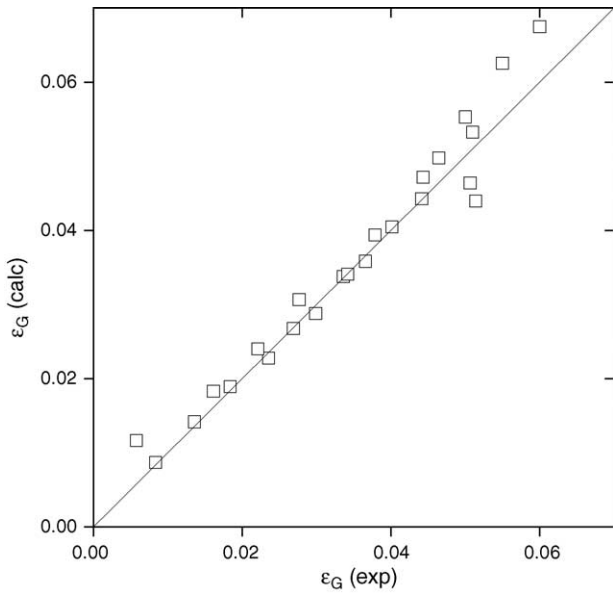


Fig. 4. Comparison of experimental and calculated (by Eq. (10)) gas volume fraction.

height, ΔP_C remains constant whereas ΔP_D increases, the importance of the latter is found to increase with the column length, as expected.

The introduction of solid particles in the riser brings about a reduction of the liquid circulation rate, this effect increasing with increasing solid loading, Fig. 6. The solid passes from fixed to the fluidised state as the gas flow rate increases, the transition corresponding in Fig. 6 to a change in gradient of the relation expressing the dependency of Q_L on Q_G . Moreover, that transition could be quite precisely detected visually, the observed values of $(Q_G)_{mf}$ being depicted in Fig. 7. The dependency of this important parameter on the solid loading

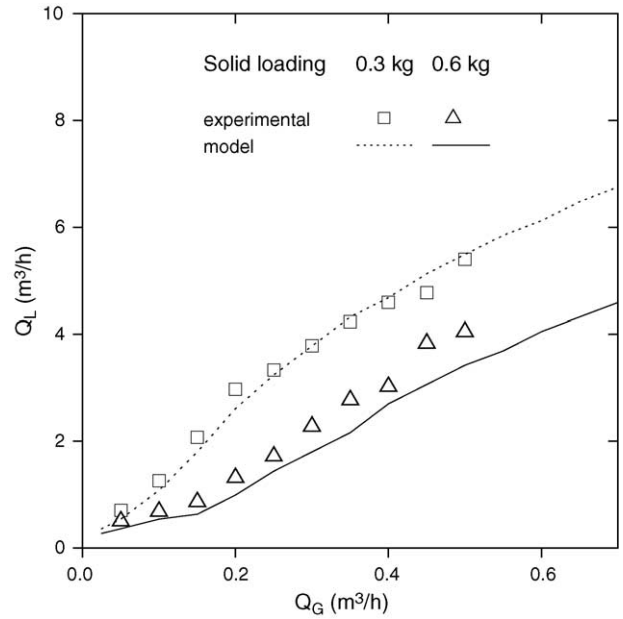


Fig. 6. Experimental and calculated liquid circulation rate function of gas flow rate. Three-phase gas–liquid–solid system.

is fully to be expected: the greater the amount of solid the greater is the resistance to the flow, so that a larger gas flow rate is needed in order to obtain the fixed liquid velocity required to fluidise the solid particles. Again the dependency of Q_L on Q_G , and the values of $(Q_G)_{mf}$, calculated using the relationships described in the previous section, agreed very well with the measured ones (Figs. 6 and 7).

Comparison between predicted and experimental solid bed expansion were also very favourable as indicated in Fig. 8. As indicated in that figure when the smaller solid

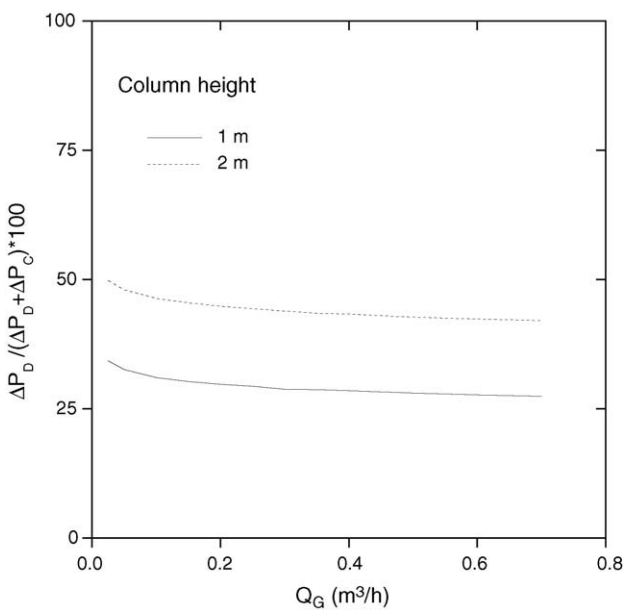


Fig. 5. The ratio of distributed pressure losses to total pressure losses.

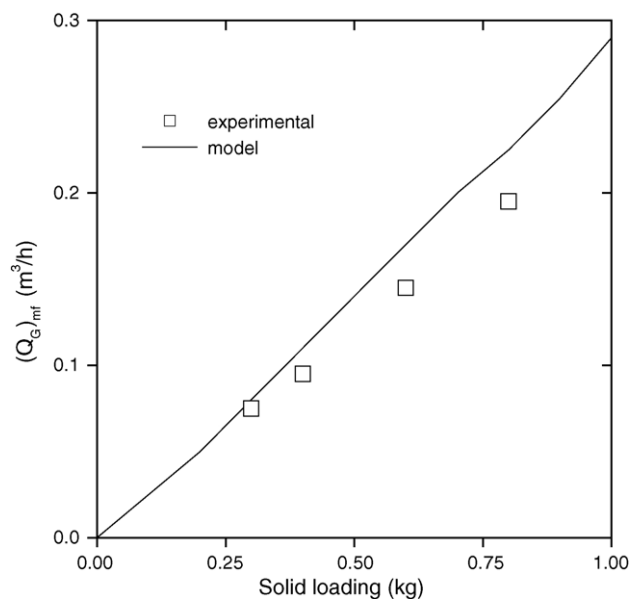


Fig. 7. Experimental and calculated gas flow rate at minimum solid fluidisation condition.

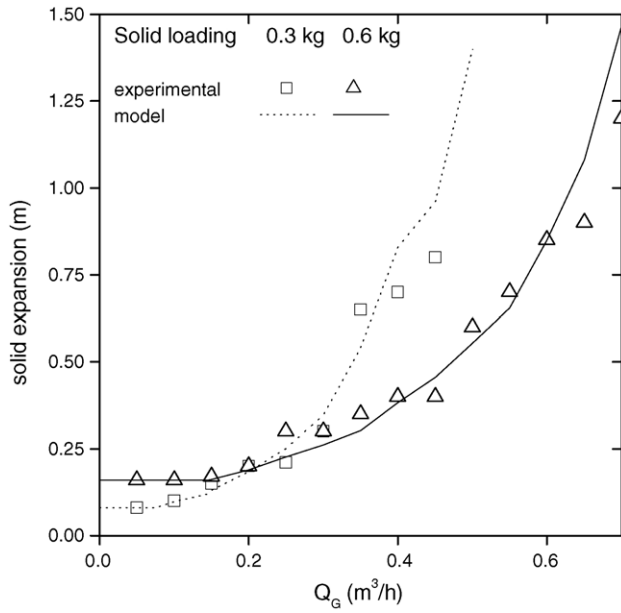


Fig. 8. Experimental and calculated solid expansion in the riser.

loading was used (0.3 kg) gas flow rate could not exceed a value of $0.5 \text{ m}^3/\text{h}$ otherwise particles would have been lost at the top of the riser and their circulation started. That threshold value increased to $0.7 \text{ m}^3/\text{h}$ for the larger solid loading (0.6 kg) as expected.

The contributions to flow resistance where solids are present are quite different to the two-phase situation. In Fig. 9 the ratio of the resistance due to the presence of the solid to the overall flow resistance is plotted for the two amounts of solid investigated, 0.3 and 0.6 kg. In both case ΔP_S represent

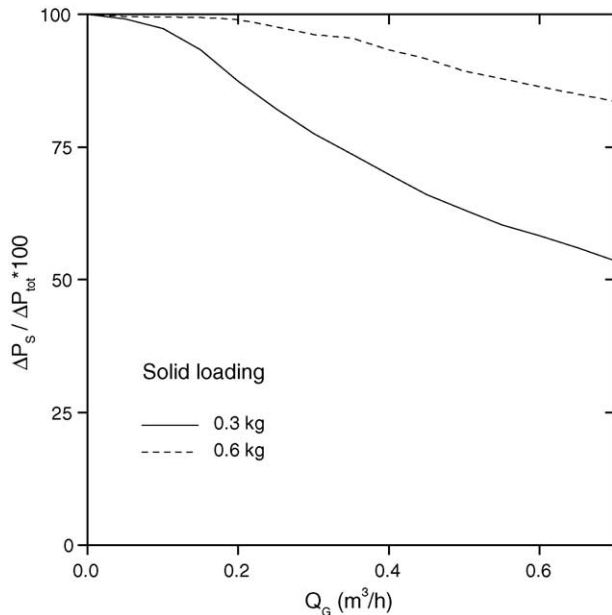


Fig. 9. The ratio of pressure losses due to the solids to total pressure losses for glass particles.

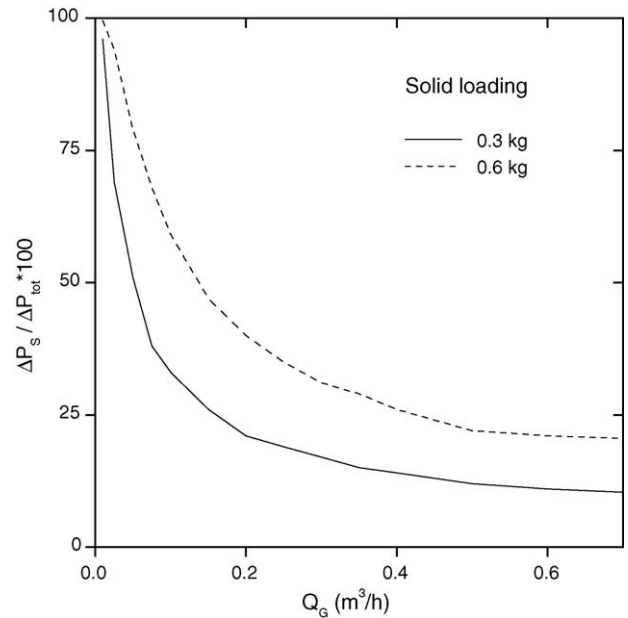


Fig. 10. The ratio of pressure losses due to the solids to total pressure losses for biomass covered particles.

the main contribution, and for the larger solid quantities is nearly 100% for the smaller gas flow rate and at least 80% of the total for the whole range reported. The shape of the curves in Fig. 9 is quite easy to justify. At low gas flow rates, with consequently low liquid circulation rates, the solid is in a fixed state; as the flow rate increases so does the resistance due to the solid particles (through the Ergun equation) which therefore remain the most important contribution. However, once the solid becomes fluidised, its pressure drop remains constant (equal to its effective weight) whereas concentrated and distributed losses continue to increase and cease to be negligible. Finally, it should be pointed out that this result is strongly dependent on the solid density, or, more precisely, on the solid effective density, $\rho_S - \rho_L$. If the solid effective density is small, as may be the case for biological systems, where the solid may even be covered with fluffy biomass, so that its density approaches that of liquid, then the piezometric pressure drop associated with the solid–fluid drag, Eq. (5), could become very small, in which case distributed and concentrated pressure losses could again become preponderant. Fig. 10 depicts such a situation: a solid of the same (5 mm) but of much smaller density (1100 kg/m^3) has been considered there and, for the higher gas flow rate, the main contribution to the total flow resistance arises from the wall–fluid frictions.

5. Conclusions

In this study we have investigated the fluid dynamic behaviour of two- and three-phase airlift reactors. Good predictions of the liquid circulation rate as a function of gas flow rate were obtained on the basis of general, independent relationships for pressure losses in multiphase flow. It was also

demonstrated that, for the gas–liquid systems, distributed and concentrated pressure losses were important, both having to be taken into account in order to predict liquid circulation rates correctly; whereas when the solid phase was introduced it came to represent the main contribution to pressure loss, rendering all other contributions negligible for most operating conditions.

Acknowledgment

The financial support of the Ministero dell'Università e della Ricerca Scientifica (MIUR) under their PRIN 2003 programme is gratefully acknowledged.

References

- [1] L.S. Fan, H.J. Hwang, A. Matsura, Hydrodynamic behaviour of a draft-tube gas-liquid-solid spouted bed, *Chem. Eng. Sci.* 39 (1984) 1677–1688.
- [2] Y.C. Hsu, M.P. Dudukovic, Gas holdup and liquid recirculation in gas-lift reactors, *Chem. Eng. Sci.* 35 (1980) 135–141.
- [3] R.A. Bello, W.R. Campbell, M. Moo-Young, Liquid circulation and mixing in an external-loop airlift reactor, *Can. J. Chem. Eng.* 62 (1984) 573–577.
- [4] M.Y. Chisti, B. Harald, M. Moo-Young, Liquid circulation in airlift reactors, *Chem. Eng. Sci.* 43 (1988) 451–457.
- [5] A.G. Livingston, S.F. Zhang, Hydrodynamic behaviour of three-phase (gas–liquid–solid) airlift reactors, *Chem. Eng. Sci.* 48 (1993) 1641–1654.
- [6] C. Freitas, M. Fialova, J. Zahradnik, J.A. Teixeira, Hydrodynamic model for three-phase internal- and external-loop airlift reactor, *Chem. Eng. Sci.* 54 (1999) 5253–5258.
- [7] E. Garcia Calvo, A fluid dynamic model for airlift loop reactors, *Chem. Eng. Sci.* 44 (1989) 321–323.
- [8] E. Garcia Calvo, A. Rodriguez, A. Prados, J. Klein, A fluid dynamic model for three-phase airlift reactors, *Chem. Eng. Sci.* 54 (1999) 2359–2370.
- [9] Ch. Vial, S. Poncin, G. Wild, N. Midoux, Experimental and theoretical analysis of the hydrodynamics in the riser of an external loop airlift reactors, *Chem. Eng. Sci.* 57 (2002) 4645–4762.
- [10] W.A.M. Bakker, H.J.L. van Can, J. Tramper, C.D. de Gooijer, Hydrodynamic and mixing in a multiple air-lift reactor, *Biotechnol. Bioeng.* 42 (1993) 994–1001.
- [11] A. Cockx, A. Liné, M. Roustan, Z. Do-Quang, V. Lazarova, Numerical simulation and physical modeling of the hydrodynamics in an air-lift internal loop reactor, *Chem. Eng. Sci.* 21/22 (1997) 3787–3793.
- [12] J.J. Heijnen, J. Hols, R.G.J.M. van der Lans, H.L.J.M. van Leeuwen, A. Mulder, R. Weltevrede, A simple hydrodynamic model for the liquid circulation velocity in a full-scale two- and three-phase internal airlift reactor operating in the gas recirculation regime, *Chem. Eng. Sci.* 52 (1997) 2527–2540.
- [13] R. Di Felice, C. Monfort Eroles, Fluid dynamic behaviour of two- and three-phase airlift reactors, *Can. J. Chem. Eng.* 81 (2003) 419–425.
- [14] R.W. Fox, A.T. McDonald, *Introduction to Fluid Mechanics*, Wiley, New York, 1998.
- [15] R. Di Felice, The pseudo-fluid model applied to three-phase fluidisation, *Chem. Eng. Sci.* 55 (2000) 3899–3906.
- [16] J.F. Richardson, W.N. Zaki, Sedimentation and fluidisation: part I, *Trans. Inst. Chem. Eng.* 32 (1954) 35–52.